Tenth U.S. National Conference on Earthquake Engineering
Frontiers of Earthquake Engineering
July 21-25, 2014
Anchorage, Alaska

AFTERSHOCK RISKS SUCH AS THOSE DEMONSTRATED BY THE RECENT EVENTS IN NEW ZEALAND AND JAPAN

Nilesh Shome[1], Nicolas Luco[2], Matt C. Gerstenberger[3], Oliver S. Boyd[4], Ned (Edward) H. Field[5], Abbie B. Liel[6] and John W. van de Lindt[7]

ABSTRACT

Recent earthquakes in New Zealand and Japan show that it is important to consider the spatial and temporal distribution of aftershocks following large magnitude events since the probability of high intensity ground motions from aftershocks, which are capable of causing significant societal impact, can be considerable. This is due to the fact that a mainshock will have many aftershocks, some of which may occur closer to populated areas and may be large enough to cause damage. When a large magnitude event strikes a region, the chance that aftershocks will cause damage can be significant as was observed after the 2011 Tohoku and 2010 Canterbury earthquakes (e.g., damage caused by M_w6.6 April 11, 2011 Fukushima-Hamadori earthquake following Tohoku earthquake or by M_w6.3 February 22, 2011 Christchurch earthquake following Canterbury earthquake). Aftershock events may further damage already damaged buildings, thereby further complicating assessments of risk to the built environment. In this paper, the issue of aftershock risk is addressed by summarizing current research regarding: (1) aftershock hazard, (2) structural fragility/vulnerability before and after the mainshock, and (3) change in risk due to aftershocks.

[1]Senior Director, Model Development, Risk Management Solutions, Newark, CA 94568
[2]Research Structural Engineer, Geologic Hazards Science Center, U.S. Geological Survey, Golden, CO 80225
[3]Risk and Engineering Team Leader, GNS Science, Lower Hutt, New Zealand
[4]Research Geophysicist, Geologic Hazards Science Center, U.S. Geological Survey, Golden, CO 80225
[5] Research Geophysicist, Geologic Hazards Science Center, U.S. Geological Survey, Golden, CO 80225
[6]Assistant Professor, Dept. of Civil, Environ. and Architectural Engineering, University of Colorado, Boulder, CO
[7]Professor, Civil and Environmental Engineering, Colorado State University, Fort Collins, CO 80523

Shome N, Luco N, Gerstenberger MC, Boyd OS, Field NH, Liel AB, and Lindt JW. Aftershok risks such as those demonstrated by the recent events in New Zealand and Japan. *Proceedings of the 10th National Conference in Earthquake Engineering*, Earthquake Engineering Research Institute, Anchorage, AK, 2014.

Tenth U.S. National Conference on Earthquake Engineering
Frontiers of Earthquake Engineering
July 21-25, 2014
Anchorage, Alaska

Aftershock Risks such as those Demonstrated by the Recent Events in New Zealand and Japan

Nilesh Shome[1], Nicolas Luco[2], Matt C. Gerstenberger[3], Oliver S. Boyd[4], Ned (Edward) H. Field[5], Abbie B. Liel[6] and John W. van de Lindt[7]

ABSTRACT

Recent earthquakes in New Zealand and Japan show that it is important to consider the spatial and temporal distribution of aftershocks following large magnitude events since the probability of high intensity ground motions from aftershocks, which are capable of causing significant societal impact, can be considerable. This is due to the fact that a mainshock will have many aftershocks, some of which may occur closer to populated areas and may be large enough to cause damage. When a large magnitude event strikes a region, the chance that aftershocks will cause damage can be significant as was observed after the 2011 Tohoku and 2010 Canterbury earthquakes (e.g., damage caused by M_w6.6 April 11, 2011 Fukushima-Hamadori earthquake following Tohoku earthquake or by M_W6.3 February 22, 2011 Christchurch earthquake following Canterbury earthquake). Aftershock events may further damage already damaged buildings, thereby further complicating assessments of risk to the built environment. In this paper, the issue of aftershock risk is addressed by summarizing current research regarding: (1) aftershock hazard, (2) structural fragility/vulnerability before and after the mainshock, and (3) change in risk due to aftershocks.

Introduction

The February 2011 Christchurch, New Zealand, aftershock of the September 2010 Canterbury earthquake or the April 2011 Fukushima-Hamadori earthquake triggered by March 2011 Tohoku-Oki earthquake are striking examples showing that hazard and risk from aftershocks or triggered events can be significant. The 2010 M_W7.1 Canterbury mainshock occurred nearly 40 km west of Christchurch, New Zealand. There was damage to unreinforced masonry structures and widespread liquefaction in Christchurch. But there was no loss of life due to the event because of limited damage to buildings. Subsequent to the earthquake, the area continued to rattle from aftershocks. Five months after the Canterbury earthquake, on February 22nd, 2011, a M_W6.2 aftershock struck Christchurch [1]. Due to the time of day and proximity to

[1]Senior Director, Model Development, Risk Management Solutions, Newark, CA 94568
[2]Research Structural Engineer, Geologic Hazards Science Center, U.S. Geological Survey, Golden, CO 80225
[3]Risk and Engineering Team Leader, GNS Science, Lower Hutt, New Zealand
[4]Research Geophysicist, Geologic Hazards Science Center, U.S. Geological Survey, Golden, CO 80225
[5]Research Geophysicist, Geologic Hazards Science Center, U.S. Geological Survey, Golden, CO 80225
[6]Assistant Professor, Dept. of Civil, Environ. and Architectural Engineering, University of Colorado, Boulder, CO
[7]Professor, Civil and Environmental Engineering, Colorado State University, Fort Collins, CO 80523

Shome N, Luco N, Gerstenberger MC, Boyd OS, Field NH, Liel AB, and Lindt JW. Aftershok risks such as those demonstrated by the recent events in New Zealand and Japan. *Proceedings of the 10th National Conference in Earthquake Engineering*, Earthquake Engineering Research Institute, Anchorage, AK, 2014.

Christchurch's central business district, there was widespread damage and loss of life. There were over 150 fatalities, complete collapse of several buildings and very high damage leading to demolition of thousands of buildings in the Central Business District area of the city.

Typically, time-independent probabilistic seismic hazard analyses (PSHA) remove the aftershocks from earthquake catalogs in order to be consistent with the conventional assumption of independent (Poissonian) earthquakes in time (as opposed to mainshock-aftershock clusters), and assume small risk from these smaller dependent events. Recent events, however, show that the increase in hazard and risk can be significant if conditioned on the occurrence of the large magnitude events. Hence, we have organized a special session at the 10th US National Conference on Earthquake Engineering to increase the awareness of aftershock risks. This paper provides an overview of the topics that are discussed in the session. The topics can be divided into three broad categories: (1) aftershock hazard, (2) change in structural fragility/vulnerability due to aftershocks, and (3) risk due to aftershocks. An extensive list of references in this paper is expected to help the interested readers gain an in-depth understanding of the wide-ranging issue of aftershock risks.

This paper provides information on the following two approaches to modeling aftershock hazard: (1) the Epidemic Type Aftershock Sequences (ETAS) model [2], summarized by Field, and (2) modeling a mainshock and associated aftershocks as a time-independent cluster [3], as summarized by Boyd. A time-dependent hazard model for the continuing Canterbury earthquake sequence for applications such as revising the local building standard is also discussed by Gerstenberger. Increases in building vulnerability due to aftershocks are demonstrated via studies of aftershock collapse fragilities of reinforced concrete (RC) buildings, by Liel, and of a two-story wood-frame building, by van de Lindt. At the end of paper, Luco describes how the information on aftershock hazard and the change in building vulnerability due to aftershocks can be combined for estimating aftershock risks.

Consideration of Earthquake Triggering in an Operational Earthquake Forecast Model for California (UCERF3)

The Working Group on California Earthquake Probabilities (WGCEP), a joint effort by the Southern California Earthquake Center (SCEC), the U.S. Geological Survey (USGS), and the California Geological Survey (CGS), has been developing the next-generation Uniform California Earthquake Rupture Forecast (UCERF version 3). Based on best-available science, UCERF3 provides authoritative estimates of the magnitude, location, and frequency of potentially damaging earthquakes in California. One of the main goals of UCERF3 is to include spatiotemporal clustering because aftershocks and triggered events can be large and damaging.

One of the challenges of including spatiotemporal clustering is that the physical process responsible for earthquake triggering remains controversial [4], and so the empirical models represent best available science. Furthermore, in forecasting earthquake ruptures there is no identifiable difference between "aftershocks" and otherwise "triggered" events, so UCERF3 does not make any distinction for those. For application of aftershocks in UCERF3, the Epidemic Type Aftershock Sequences (ETAS) model [2], which is a generalization of well-known empirical aftershock statistics (e.g., Omori's law), has been adopted. In ETAS, every earthquake can spawn its own aftershocks, leading to aftershocks of aftershocks, then aftershocks to those aftershocks, etc. It turns out that such non-direct triggering is important for getting broad enough spatial and temporal influence, such as having the Hector Mine earthquake sequence triggered

several years and several kilometers away from the Landers mainshock.

Implementing the ETAS model has raised several interesting scientific issues. First, it implies that UCERF2 (the previous long-term model) [5] has regional magnitude frequency distributions that were far too characteristic (in a non-Gutenberg-Richter sense). For example, in a region surrounding the 1994 Northridge earthquake, UCERF2 predicted that the likelihood of having an ~M_w6 earthquake is about the same as having an ~M_w5 event. This produces runaway aftershock sequences (never ending), implying the UCERF2 long-term model is questionable.

Another interesting and surprising issue is that ETAS requires the inclusion of elastic rebound in order to reduce the probability that a just-ruptured fault will rupture again [6]. For example, the manifestation of excluding elastic rebound in previous attempts to model spatiotemporal clustering [7] leads to the highest probability of having the "big one" on the San Andreas Fault being the moment after it occurs. The fact that we do not see large events immediately re-rupturing the same fault section in nature implies that elastic rebound is required. Another UCERF3 improvement is that aftershocks are sampled from the exact same population of events that exists in the long-term model, so that, for example, an ~M_w8 event can only be triggered where there is a fault capable of producing such an event.

The intent of UCERF3 is to provide the basis for an operational earthquake forecasting system in California, now listed as one of the strategic-action priorities of the USGS in terms of providing "effective situational awareness" during hazardous events (http://pubs.usgs.gov/of/2012/1088; page 31).

Earthquake Hazard from Both Independent and Dependent Events

Boyd [3] presents a method to estimate the hazard due to both mainshock and dependent events. The mainshock and its dependents are considered as a time-independent cluster, each cluster being independent from any other. The cluster has a recurrence time of the mainshock, and each earthquake in the cluster has an opportunity to exceed a given level of ground motion. At annual rates of exceedance close to the annual rate of the cluster, the mainshock dominates the hazard. However, as rates of annual exceedance decrease, the contribution to hazard from dependent events increases.

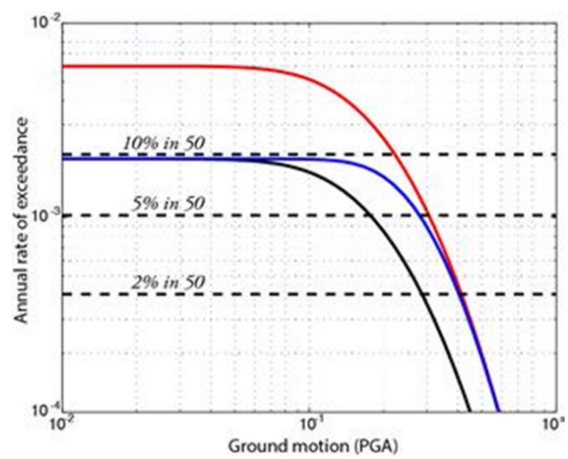

Figure 1. The effect of clustering on a hazard curve for a site located equidistant from three New Madrid-type earthquakes. The black curve is a single event, the red curve, three independent events, and the blue curve, a clustered analysis.

Toro and Silva [8] proposed this type of cluster for the 1811–1812 New Madrid-type sequence of events. Fig. 1 shows hazard curves for a site equidistant from three New Madrid earthquakes. For return periods on the order of the return period of the cluster, 500 years, hazard appears to result from a single event. There is a high probability that one of the events will exceed the given ground motion. But at longer return periods, the probability that any individual event within the cluster will exceed the higher ground motion decreases. The hazard curve then approaches the case where each event contributes independently to hazard. For a scenario like

New Madrid and a site equidistant from the New Madrid earthquakes, hazard for the ground motions expected to be exceeded with a 2% probability in 50 years increases by ~40%.

Unlike the New Madrid series of events in which all three earthquakes were of similar magnitude, foreshocks and aftershocks are in general: (1) smaller than the mainshock by, on average, at least one magnitude unit, and (2) more numerous. For a high hazard site near the San Andreas Fault in central California, including dependent events causes ground motions that are exceeded at probability levels of engineering interest to increase by about 10 percent, but this increase could be as high as 20 percent if variations in aftershock productivity can be accounted for reliably (Fig. 2). At lower hazard sites, the contribution from dependent events is less significant, which is true in general.

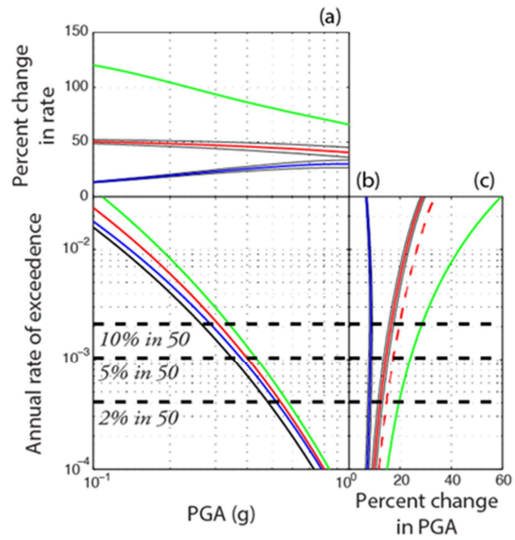

Figure 2. Ground motion hazard for San Jose, CA. (a) Changes in annual rates (b) Hazard curves and (c) change in ground motions. Black curves in (b) represent a traditional analysis with a declustered catalog, green curves for a traditional analysis using the original non-declustered catalog, red curves for a full catalog where foreshocks and aftershocks are synthesized and have either a uniform azimuthal distribution (solid curves) or are distributed along an azimuth of N45W (dashed curves) and all events are treated independently, and blue curves for an analysis where the mainshocks and associated foreshocks and aftershocks are treated as a cluster and have a uniform azimuthal distribution.

Time-Dependent Hazard for Canterbury, New Zealand and Modeling of Expected Ground Motions

Gerstenberger and colleagues have developed a time-dependent hazard model for the continuing Canterbury earthquake sequence. This hazard model has been used for applications such as revising the building standard and planning for rock-fall potential. An important consideration in the development of this hazard model has been the underpinning ground motion predictions which have been determined using existing and modified ground motion prediction equations (GMPEs). To provide additional insight into expected ground motions in the Canterbury region, broadband ground motion simulations have been carried out using a suite of moderate sized aftershocks (M_w5.3+) from the Canterbury sequence. These simulations are used to investigate the sensitivity of near field ground motions to key engineering parameters including stress drop and rupture details such as velocity, directivity and slip distribution. The synthetic seismograms and the corresponding response spectra are modeled by employing the EXSIM code [9].

Source Models

The Canterbury earthquake ruptures have been extensively studied using strong motion data [10, 11], GPS, InSAR data and teleseismic data. For the M_w6.2 February 22nd 2011 event, the source model of Holden [10] is employed (details can be found in [28]). For the M_w6.0 June 13th 2011 and M_w5.9 December 23rd 2011 events, source models as described in Holden and Beavan [11] are used. The shallow M_w5.3 aftershock located near the epicenters of the February and June events are also included. This event—with a relatively moderate magnitude— triggered

landslides and rock falls in the Port Hills.

Stress Drop, Attenuation and Quantification of Site Effects

Key regional parameters used to guide the ground motion modeling have been derived using spectral inversion of the extensive Canterbury strong motion dataset [12]. These include: (1) a regional frequency-dependent attenuation relationship; (2) stress drop estimates for each source; and (3) site-specific horizontal and vertical frequency-dependent amplification functions. The adoption of these parameters provides an improved and robust fit to the observed data. This fact emphasizes the need for region-specific considerations in the development of GMPEs.

To start with, the standard rock site ground motions in Canterbury, i.e., without site effects, is modeled. This is done by adopting the horizontal and vertical site amplification functions for rock site D14C [12], which serves as an appropriate rock reference station. In a second stage the site-specific ground motions are computed by adopting the relevant amplification functions derived at each site under linear soil behavior. Results show that using the appropriate stress drop value and site specific amplification function helps greatly to reproduce key parameters such as Peak Ground Acceleration (PGA) and response spectra.

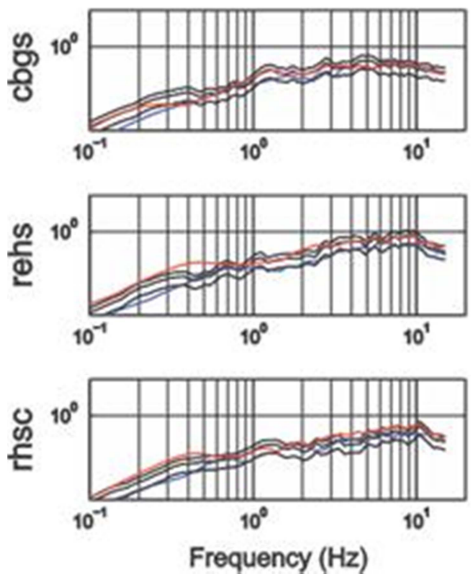

Figure 3: Spectral acceleration (5% damping) for vertical components of recorded (black) ground motions in Christchurch following the M_w5.9 December 23rd 2011 earthquake. The dashed lines represent 50% standard deviation of the recorded acceleration spectra. The blue lines represent synthetic ground motions for rock site conditions; the red lines are synthetic ground motions for site specific conditions including a frequency-dependent amplification function. The green lines are response spectra from the McVerry et al. model [13].

Fig. 3 presents comparisons of response spectra for the M_w5.9 December 23rd 2011 earthquake of the recorded motions with those from different cases. Whereas the GMPE-derived model provides a smooth overall estimate of the response spectra, the frequency-dependent, site-specific synthetic models reproduce more realistic response spectra throughout the whole frequency band. Preliminary analysis shows favorable results when the simulations are compared to the GMPE [13] used in the time-dependent Canterbury seismic hazard model.

Aftershock Collapse Fragilities for Mainshock-Damaged RC Frame Buildings

Liel and colleagues use nonlinear building simulation models to quantify the impact of mainshock building damage on a structure's capacity to withstand subsequent (aftershock) ground shaking. The analysis is based on 4 RC frame structures varying in height from 2 to 12 stories, which have been designed and detailed according to modern U.S. seismic design codes for southern California. Although these buildings have a low probability of collapse under a design-level earthquake event [14], damage to structural elements may occur in large earthquakes [15], potentially increasing their vulnerability in an aftershock.

The buildings are modeled as two dimensional frames in OpenSees [16]. To quantify the response of a building in the event of an earthquake or a sequence of earthquakes, incremental dynamic analysis (IDA) is carried out on the nonlinear building model. Ground motion intensity is quantified by the inelastic spectral displacement at the fundamental period of the structure, denoted S_{di} [17].

As the first step in the analysis, IDA is carried out on the modeled intact buildings. In aftershock analysis, the building is subjected to a mainshock-aftershock (MS-AS) sequence. The MS record is scaled to achieve a particular damage state in the structure and, subsequently, an AS record is applied to the MS-damaged structure. The AS analysis is conducted with increasing scale factors on the AS ground motion until the building collapses in the aftershock. The aftershock IDA is used to determine the collapse capacity of the MS-damaged building. MS-AS sequences for this analysis are generated using a set of 30 ground motions [18] for a total of 900 earthquake sequences.

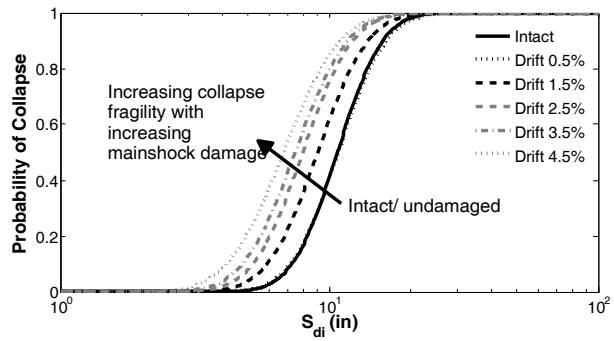

Figure 4. Fragility curves for a 4-story building damaged to certain damage levels in mainshock.

The fragility curves calculated for the 4-story building with varying levels of damage in the mainshock (corresponding to maximum interstory drift ratios of 0.5% to 5%) are shown in Fig. 4, and compared with the collapse fragility curves for the intact building, illustrating the types of results that are possible through such an analysis. Low or moderate damage does not signficantly alter a building's fragility to aftershock events. However, the difference in fragility between the damaged and intact buildings becomes more significant as buildings experience more damage. Similar findings are also observed for the other buildings.

These results can be used to identify the indicators of physical damage in the mainshock that most strongly signify a reduction in capacity to withstand subsequent events. This information is useful in the context of visual post-earthquake safety evaluation procedures such as ATC-20 [19]. This study examines a number of damage indicators ranging from residual drift, number of damaged beams and columns, to maximum interstory ratio (IDR) or roof drift. Among these the maximum IDR (shown in Fig. 5) and maximum roof drift during the mainshock are the best indicators of reduced capacity for subsequent events. However, residual IDR and roof drifts are also strong predictors of fragility in the context of future earthquake events, and these indicators are readily obtained through a post-earthquake visual inspection.

Effect of Aftershock Intensity on Seismic Collapse Fragilities

Van de Lindt and colleagues have investigated the effect of spatial distribution of aftershocks in a rupture zone on structures by computing the collapse probability of a modeled two-story woodframe mainshock-damaged building. The variation of mainshock-aftershock (MS-AS) fragilities is used to determine the effect of aftershock intensity on collapse probability. Building nonlinear response data is obtained from NEEShub (www.nees.org) for a two-story woodframe townhouse [20], and a two degree-of-freedom numerical collapse model is calibrated to the story hysteresis. The completed building with drywall and stucco was used in the present study since

this would be the building in its in-situ state. The natural period of the building was 0.21 seconds. A 10-parameter CASHEW hysteretic spring model [21] was fit to the global hysteresis measured during the MCE level (Los Angeles, California; 1.8g spectral acceleration (S_a) at 0.21 sec.) tri-axial shake using the 1994 M_W6.7 Northridge earthquake ground motion record from the Rinaldi Electrical Substation Los Angeles Department of Water and Power (LA DWP) Rinaldi Receiving Station #77.

In the present case, the seismic intensity is varied due to site-to-source distance as modified from an attenuation equation [22]. This is accomplished by scenarios of MS-AS analysis for a hypothetical site in California. It is assumed that a mainshock of M_w7.3 occurs 10 kilometers from the site. The magnitude of the aftershock is set to a constant value of M_w6.7, and the aftershocks are located at 5 and 25 kilometers away from the site. The incremental dynamic analysis (IDA) for the spatial distribution of the mainshock and aftershocks is carried out by using a sequence of ground motions for those events. Fig. 6 shows the normalized collapse fragilities (normalized to 8g S_a) for the 1990's style woodframe building in southern California for the MS-AS scenarios as well as for the mainshock only.

Inspection of Fig. 6 shows that at 0.2 normalized S_a, which corresponds to approximately the MCE in Los Angeles, i.e. 1.6g, the collapse probability is approximately 13% for the mainshock. If the MS-AS occurs with the aftershock moving close to 5 km, the collapse probability increases to 60%. Although the ground motions, distances, magnitudes and fault characteristics are not the same as the scenario that occurred in Christchurch in 2010 and 2011, one can see the drastic effect on collapse probability that results from an aftershock if it moves closer to a building [23].

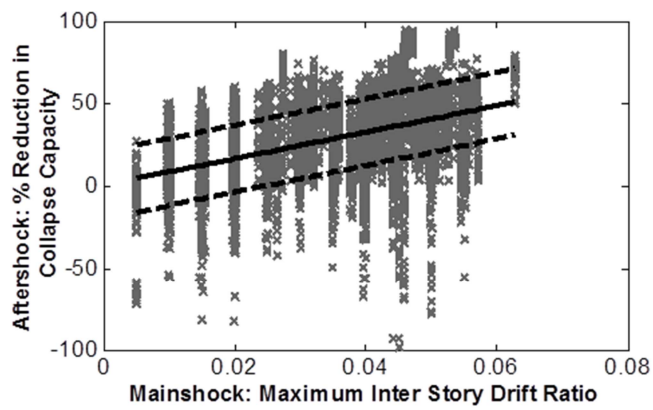

Figure 5. Percent reduction in collapse capacity, as a function of mainshock damage as quantified by maximum interstory drift.

Aftershock Risk Assessment

Increasingly, probabilistic seismic risk (of damage) assessment is becoming the basis for longer-term or "pre-earthquake" mitigation approaches for buildings and other structures, e.g., seismic design standards in building codes. For example, the latest edition of the International Building Codes [24] defines Risk-Targeted Maximum Considered Earthquake (MCE_R) ground motion maps for the United States by explicitly targeting a probabilistic 1% risk of collapse in 50 years, which is an approximation of the lifespan of a building.

Probabilistic risk assessment has also been proposed as a basis for making shorter-term or "post-earthquake" mitigation decisions after a mainshock (or any other earthquake) has occurred and when the threat of aftershocks (or other triggered earthquakes) lingers. For example, the Advanced Seismic Assessment Guidelines developed by Bazzurro et al. [25] use the probability that an aftershock ground motion exceeds the capacity of a mainshock-damaged building as a rational criterion for deciding whether and when to permit re-occupancy of the building. Similarly, Yeo and Cornell [26] have developed a time-dependent building "tagging" (i.e., permitting or restricting occupancy) policy for the aftershock environment using probability of collapse as a proxy for fatality risk. Luco et al. [27] have presented a similar methodology for

post-earthquake probabilistic risk assessment in order to develop a computational tool for automatic or semi-automatic assessment that can inform emergency response mobilization, inspection prioritization, and re-occupancy decisions. In either case (pre- or post-earthquake), the probabilistic risk assessments have two main components: (i) ground motion hazard information for the location of a structure of interest, and (ii) knowledge of the fragility/vulnerability of the structure with respect to potential ground motion intensities.

For pre-earthquake mitigation approaches (e.g., building codes or insurance/reinsurance) that are based on probabilistic risk assessment, the following models discussed in the sections above can be applied in order to account for aftershocks:

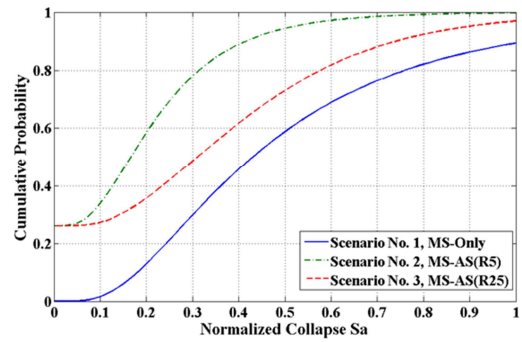

Figure 6. Total collapse probabilities vs. spectral acceleration (S_a) curves for three different scenarios.

- The method discussed in the section entitled "Earthquake Hazard from Both Independent and Dependent Events" can be applied in order to include aftershocks (and foreshocks) in the ground motion hazard component of the risk assessment. Typical pre-earthquake hazard assessments deliberately exclude aftershocks.
- The medium- and long-term time-dependent hazard models mentioned in the section entitled "Time-Dependent Hazard for Canterbury, New Zealand …" can also be used in order to include earthquake clustering (e.g., of mainshocks and aftershocks) in the hazard component of the risk assessment, as has already has already been done for Canterbury.
- Scenario mainshock-aftershock building fragilities like those demonstrated in the section entitled "Effect of Aftershock Intensity on Seismic Collapse Fragilities," when combined with numerous other such scenario fragilities, can be used to account for aftershocks (or other triggered earthquakes) in the building fragility/vulnerability component of the risk assessment. Typical building fragilities only account for intact structures subject to mainshocks and do not account for damaged structures subject to aftershocks.

Furthermore, the following models discussed in the previous sections can be applied in order to account for aftershocks in *post-earthquake* mitigation decisions (e.g., inspection prioritization and re-occupancy decisions) that are based on *post-earthquake* probabilistic risk assessment:

- The operational earthquake forecast model described in the section entitled "Consideration of Earthquake Triggering in an …" can be combined with ground motion models (such as those discussed in the "Time-Dependent Hazard for Canterbury, New Zealand …" section) in order to include, in near-real time, spatiotemporal clustering (e.g., of mainshocks and aftershocks) in the hazard component of the post-earthquake risk assessment. Typical hazard assessments are not updated immediately after a mainshock occurs.
- The short-term time-dependent hazard models mentioned in the section entitled "Time-Dependent Hazard for Canterbury, New Zealand …" can also be used in order to include earthquake clustering in the hazard portion of the post-earthquake risk assessment.
- As alluded to in the section entitled "Aftershock Collapse Fragilities for Mainshock-Damaged RC Frame Buildings," such aftershock fragilities can be used for the building fragility/vulnerability component of the post-earthquake risk assessment, since they account

for damage from the preceding earthquakes.

Conclusion

In this paper, three different approaches for calculating aftershock hazard and two approaches for estimating increased collapse probability of buildings due to aftershocks have been discussed. These approaches can be synthesized to compute the increased earthquake risk of damage or collapse of buildings following earthquakes. This paper provides an overview of the topics discussed in the special session on aftershocks in the 10th U.S. National Conference on Earthquake Engineering to help researchers considering aftershocks explicitly in risk calculations. A long list of references, written by many of the contributing authors of this paper, is expected to provide additional information to researchers and interested readers.

Acknowledgments

We appreciate the reviews of Morgan Page, Kishor Jaiswal, Mark Petersen, Jill McCarthy, Janet Slate and an anonymous reviewer, which helped to improve the clarity of this paper. Funding for the study of RC buildings was provided through the U.S. Geological Survey Cooperative Agreement #G10AC00100. This study would not have been possible without the contributions of University of Colorado Boulder graduate student M. Raghunandan, as well as collaborators H. Ryu and S.R. Uma. Funding for the light-frame wood example was provided through the National Science Foundation grant CMMI-1100423 through a subcontract from Michigan Technological University to Colorado State University (CSU). The collaboration of Prof. Y. Li as PI on the project and CSU graduate student N. Nazari is acknowledged. The study of time-dependent hazard for Canterbury is in collaboration with C. Holden and A. Kaiser of GNS science, New Zealand. The opinions contained herein do not necessarily represent those of Risk Management Solutions.

References

1. Kaiser A, Holden C, Beavan J, et al. The Mw 6.2 Christchurch earthquake of February 2011: preliminary report. *New Zealand Journal of Geology and Geophysics* 2012. **55**(1): 67–90.
2. Ogata Y. Statistical models of point occurrences and residual analysis for point processes, *J. Am. Stat. Assoc.* 1988, **83**: 9-27.
3. Boyd OS. Including Foreshocks and Aftershocks in Time-Independent Probabilistic Seismic-Hazard Analyses. *Bulletin of the Seismological Society of America* 2012. **102**(3): 909−917.
4. Felzer KR and Brodsky EE. Decay of aftershock density with distance indicates triggering by dynamic stress. *Nature* 2006, **441**.
5. Field EH, Dawson TE, Felzer KR, et al. Uniform California Earthquake Rupture Forecast, Version 2 (UCERF 2), *Bulletin of the Seismological Society of America 2009*. **99**: 2053-2107.
6. Field EH. Aftershock statistics constitute the strongest evidence for elastic relaxation in large earthquakes – Take 2 (abstract). *Seismological Research Letter* 2012, **83**(369).
7. Gerstenberger M, Wiemer S, Jones LM, and Reasenberg PA. Real-time forecast of tomorrow's earthquakes in California. *Nature* 2005, **435**:328-331.
8. Toro, GR, and Silva WJ. Scenario earthquakes for Saint Louis, MO, and Memphis, TN, and seismic hazard maps for the central United States region including the effect of site conditions, *USGS Contract 1434-HQ-97-GR-02981:* Reston, VA, 2001. (http://www.riskeng.com/PDF/Scen_CEUS_Rept.pdf)
9. Motazedian D, and Atkinson GM. Stochastic finite-fault modelling based on a dynamic corner frequency.

Bulletin of the Seismological Society of America 2005. **95**: 995-1010.

10. Holden C. Kinematic source model of the 22 February 2011 Mw 6.2 Christchurch Earthquake using strong motion data. *Seismological research letters* 2011. **82**(6): 783-788; doi: 10.1785/gssrl.82.6.783
11. Holden C and Beavan J. Source studies of the ongoing (2010-2011) sequence of recent large earthquakes in Canterbury, *Proceedings of the 15th World Conference on Earthquake Engineering* (15WCEE), Lisbon, Portugal, September 24-28, 2012.
12. Kaiser AE, Oth A, Benites RA. Source, path and site effects influencing ground motions during the Canterbury earthquake sequence, determined from spectral inversions. Paper 18: *Proceedings of the New Zealand Society for Earthquake Engineering Annual Meeting*, 26 – 28 April, Wellington, 2013.
13. McVerry GH, Zhao JX, Abrahamson NA, and Somerville PG. Response spectral attenuation relations for crustal and subduction zone earthquakes. *Bull. New Zeal. Soc. Earthquake Eng* 2006. **39**: 1–58.
14. Haselton, CB, Liel AB, Deierlein GG, et al. Seismic Collapse Safety of Reinforced Concrete Buildings. I: Assessment of Ductile Moment Frames. *Journal of Structural Engineering* 2011. **137**: 481.
15. Ramirez CM, Liel AB, Mitrani-Reiser J, et al. Expected earthquake damage and repair costs in reinforced concrete frame buildings. *Earthquake Engineering & Structural Dynamics* 2012. **41**(11): 1455–1475.
16. OpenSees. Open System for Earthquake Engineering Simulation. http://opensees.berkeley.edu/ (last accessed Oct. 6, 2013).
17. Tothong P, and Cornell CA. An empirical ground-motion attenuation relation for inelastic spectral displacement. *Bulletin of the Seismological Society of America* 2006. **96**(6): 2146–2164.
18. Vamvatsikos D, and Cornell CA. Direct estimation of the seismic demand and capacity of oscillators with multi-linear static pushovers through IDA. *Earthquake Engineering & Structural Dynamics* 2006. **35**(9): 1097−1117.
19. ATC-20. *Procedures for Postearthquake Safety Evaluation of Buildings & Addendum*. Applied Technology Council: Redwood City, California, 2005.
20. Filiatrault A, Christovasilis I, Wanitkorkul A, and Lindt, JW van de. Experimental Seismic Response of a Full-Scale Light-Frame Wood Building. *ASCE Journal of Structural Engineering* 2010, **136**(3), 246-254.
21. Folz B, and Filiatrault A. Cyclic analysis of wood shearwalls. *ASCE J. Struct. Eng*. 2001. **127**(4): 433-441.
22. Abrahamson NA and Silva WJ. Empirical Response Spectral Attenuation Relations for Shallow Crustal Earthquakes. *Seismological Research Letters* 1997. **68**(1), 94-127.
23. Nazari N, Lindt JW van de, and Li Y. Effect of Aftershock Intensity of Seismic Collapse Risk of Existing Woodframe Buildings. Submitted to the *International Journal of Reliability and Safety*: Special Issue on Robust Engineering Solutions with Environmental Loading, 2014.
24. IBC. International Building Code. *International Code Council*: Washington, DC, 2012.
25. Bazzurro P, Cornell CA, Menun C, et al. Advanced Seismic Assessment Guidelines. *Pacific Earthquake Engineering Research Center* Report 2006, PEER 2006/05: Berkeley, CA.
26. Yeo G and Cornell CA. Stochastic Characterization and Decision Bases under Time-Dependent Aftershock Risk in Performance-Based Earthquake Engineering. *Pacific Earthquake Research Center* 2005, PEER 2005/13: Berkeley, CA.
27. Luco N, Gerstenberger MC, Uma SR, et al. A Methodology for Post-Mainshock Probabilistic Assessment of Building Collapse Risk. *Proceedings of the 9th Pacific Conference on Earthquake Engineering* 2011.
28. SRL Focused Issue. The 22 February 2011 Magnitude 6.2 Christchurch Earthquake. *Seismological Research Letters* 2011. 82(6), 761-991.